



Parameters optimization defined by statistical analysis for cysteine–dextran radiolabeling with technetium tricarbonyl core

Eutimio Gustavo Fernández Núñez^{a,*}, Bluma Linkowski Faintuch^a, Rodrigo Teodoro^a, Danielle Pereira Wiecek^a, Natanael Gomes da Silva^a, Minas Papadopoulos^b, Maria Pelecanou^c, Ioannis Pirmettis^b, Renato Santos de Oliveira Filho^d, Adriano Duatti^e, Roberto Pasqualini^f

^a Radiopharmacy Center, Institute of Energetic and Nuclear Research, Sao Paulo, SP 05508-000, Brazil

^b Institute of Radioisotopes, Radiodiagnostic Products, National Center for Scientific Research 'Demokritos', Athens, Greece

^c Institute of Biology, National Center for Scientific Research 'Demokritos', Athens, Greece

^d Faculty of Medicine, Federal University of Sao Paulo, SP, Brazil

^e Department of Radiological Sciences, University of Ferrara, Ferrara, Italy

^f CIS Bio International, Gif sur Yvette, France

ARTICLE INFO

Article history:

Received 12 November 2009

Received in revised form

2 January 2011

Accepted 3 January 2011

Available online 8 January 2011

Keywords:

[^{99m}Tc(OH₂)₃(CO)₃]⁺ precursor

Technetium

Radiolabeling

Experimental design

Dextran

Statistical analysis

ABSTRACT

The objective of this study was the development of a statistical approach for radiolabeling optimization of cysteine–dextran conjugates with Tc-99m tricarbonyl core. This strategy has been applied to the labeling of 2-propylene–S–cysteine–dextran in the attempt to prepare a new class of tracers for sentinel lymph node detection, and can be extended to other radiopharmaceuticals for different targets. The statistical routine was based on three-level factorial design. Best labeling conditions were achieved. The specific activity reached was 5 MBq/μg.

Crown Copyright © 2011 Published by Elsevier Ltd. All rights reserved.

1. Introduction

Dextran are biopolymers composed of linear α-1,6-linked D-glucopyranose units with low percentage of linked side chains (Šević and Pantelić, 2008; Sun and Chu, 2006). They are easily soluble, biodegradable, nontoxic and can be obtained in a variety of molecular weights (1000–2,000,000 Da by enzymatic hydrolysis) (Sun and Chu, 2006; Castellanos et al., 2008). These polysaccharides are used as important reagents in a broad range of synthesis in biotechnological and technical industries (Khalikova et al., 2005; Heinze et al., 2007; Krishnamoorthi et al., 2007).

Dextran solutions for injection are commonly used in clinical practice for replacement of blood loss, plasma substitution in hypotension or shock, prophylaxis of thromboembolism, volume expansion and rheological improvement (de Belder, 1996). They have also been used as drug carriers or as carriers of radionuclides.

Technetium-99m-dextran were evaluated as diagnostic agents for different nuclear medicine techniques such as angiocardiology, lymphoscintigraphy, inflammation and protein losing enteropathy imaging (Matsunaga et al., 2005).

^{99m}Tc-dextran 500 and ^{99m}Tc-dextran-70 have been used for some years for lymphoscintigraphic applications, along with other radiopharmaceuticals, most of them are colloids. The most used tracers for lymph node detection are ^{99m}Tc-sulfur colloid, and ^{99m}Tc-human serum albumin (Schauer et al., 2005).

In recent years, many imaging studies were conducted by Positron Emission Tomography (PET) and the combined technique PET–Computed Tomography (CT), employing the PET tracer ¹⁸Fluoro-2-deoxyglucose ([¹⁸F]FDG). These techniques are valuable for evaluating dimension of lymph nodes, one of the criteria of malignant invasion, although even normal-sized nodes may be infiltrated. In principle, PET permits the recognition of positive lymph nodes regardless of size, but has limited sensitivity in detecting microscopically small tumors. Spatial resolution is an important factor, and most PET scanners do not have sufficiently high resolution to enable detection of micrometastases (Avril et al., 2005; El-Maraghi and Kielar, 2008; Zornoza et al., 2004).

* Corresponding author. Tel.: +55 11 31339558.

E-mail address: eutimiocu@yahoo.com (E.G. Fernández Núñez).

This deficiency justifies the continued utilization of ^{99m}Tc -based products as radiopharmaceuticals of choice for lymph node scintigraphy. Various options are commercially available such as Nanocis (bioCis International—IBA) (Bensimhon et al., 2008) and Lymphoseek (Neoprobe Corp., Dublin, OH) (Wallace et al., 2003).

Since the first publications of Alberto and coworkers (1998) on six-coordinated Tc(I) tricarbonyl complexes, this chemical modality has been intensively used for designing new ^{99m}Tc radiopharmaceuticals due to high stability of the resulting complexes. GMP-compliant kits for the preparation of $[\text{}^{99m}\text{Tc}(\text{OH}_2)_3(\text{CO})_3]^+$ are now commercially distributed (Mundwiler et al., 2005).

The three aqua ligands of the *fac*- $[\text{}^{99m}\text{Tc}(\text{OH}_2)_3(\text{CO})_3]^+$ synthon are labile and readily substituted by several functional groups including amines, thioethers, imines, thiols, carboxylates and phosphines, with the purpose of achieving stable coordinated complexes (Kyprianidou et al., 2009; Alberto, 2005). S-Functionalized cysteine and homocysteine contains functional groups of thioether, carboxyl, and amino group that are efficient for ^{99m}Tc chelating. (van Staveren et al., 2005; Karagiorgou et al., 2005).

In the course of all such labeling procedures, optimization is an essential but cumbersome step. Routines for simplifying its complexities, at the same time improving reproducibility and reliability would be advantageous.

The objective of this study was the development of a statistical strategy for radiolabeling optimization of cysteine–dextran conjugates with technetium-99m tricarbonyl core. The basic hypothesis was that a three-level factorial design, widely employed in pharmaceutical and chemical studies but essentially untested within the radiopharmaceutical context, could successfully contribute to optimization maneuvers. The possibility of application to other radiopharmaceuticals that rely on cysteine dextran as carrier was also envisaged.

2. Materials and methods

2.1. Materials

$\text{Na}[\text{}^{99m}\text{TcO}_4]$ was eluted from $^{99}\text{Mo}/\text{}^{99m}\text{Tc}$ generator (Institute of Energetic and Nuclear Research, IPEN/CNEN-SP, Brazil), using 0.9% saline. $[\text{}^{99m}\text{Tc}(\text{OH}_2)_3(\text{CO})_3]^+$ was prepared from Isolink kit (Tyco Healthcare, St. Louis, MO, USA).

2-propylene–S–cysteine–dextran with chemical purity higher than 95% (Fig. 1) was provided without cost by National Center for Scientific Research “Demokritos” Athens, Greece (MW 16,600 Da). It is composed by 73 units of glucose and 30 of cysteine.

Vital dye for combined technique (patent blue V) was purchased from Guerbet Prod. Radiológicos Ltd., Rio de Janeiro, RJ, Brazil.

Six young female *Wistar* EPM-1 rats (150–200 g) were provided by the Animal Facility of IPEN-CNEN. They were kept in cages with controlled temperature, humidity and noise, receiving industrialized chow and water ad libitum. Current protocol was approved by the Animal Welfare Ethical Committee.

2.2. Preparation of the precursor $[\text{}^{99m}\text{Tc}(\text{OH})_3(\text{CO})_3]^+$

$[\text{}^{99m}\text{Tc}(\text{OH}_2)_3(\text{CO})_3]^+$ was prepared from Isolink kit, adding 1 ml (925 MBq) of $\text{Na}[\text{}^{99m}\text{TcO}_4]$ and heating at 100 °C for 20 min. The reaction was stopped by placing the flask in ice bath and pH was neutralized with 300 μL of 1 M phosphate buffer/HCl 1N (1:2).

2.3. Quality control

Radiochemical purity of ^{99m}Tc -2-propylene–cysteine–dextran was routinely determined using a combination of thin layer and paper chromatography. Thin layer chromatography (TLC) was

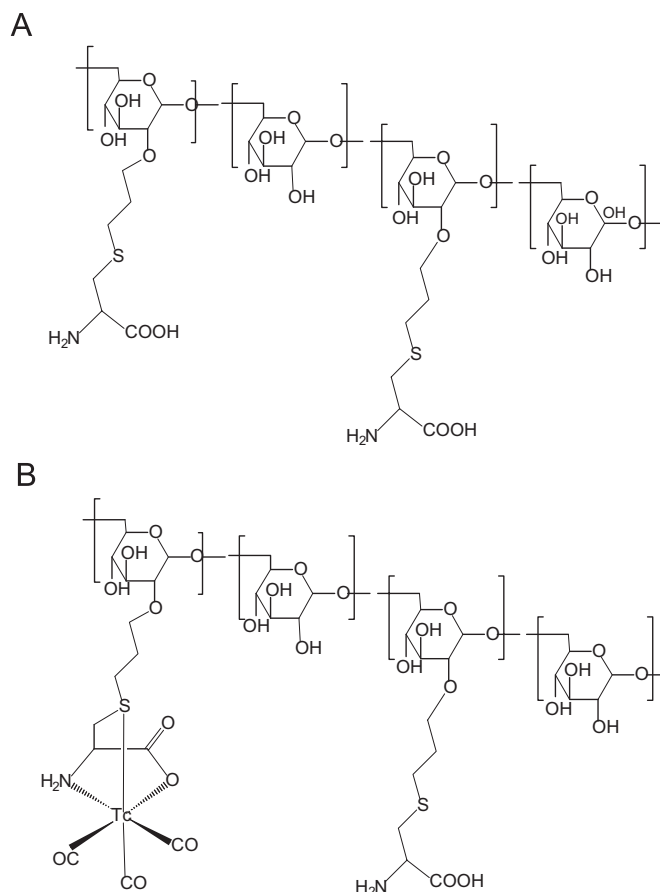


Fig. 1. Chemical structure of modified dextran (2-propylene–S–cysteine–dextran) (A) and proposed structure of its technetium-99m complex (B).

carried out using silica gel impregnated glass fiber sheets (10 cm) supplied by Pall Corporation, Ann Arbor, MI, USA, with Methanol/HCl (99:1). Paper chromatography was performed on Whatman 1 paper, UK (10 cm), with acetone. Radioactive profile of ITLC and paper strips was measured in AR-2000 radio-Thin-Chromatography Imaging Scanner (Bioscan, NW, USA).

Gel filtration chromatography was performed on a PD-10 Column to confirm radiochemical purity. Bed volume and height of the column were 9.1 mL and 5 cm, respectively. Sample (0.1 mL) was loaded and eluted with distilled water. Forty consecutive fractions (0.5 mL) were collected and radioactivity was determined by γ counting. The dextran conjugate was also characterized by reverse-phase high performance liquid chromatography (RP-HPLC), including $[\text{}^{99m}\text{Tc}(\text{OH}_2)_3(\text{CO})_3]^+$ precursor. Analysis was performed on LC-10 AT VP Liquid chromatograph (Shimadzu, Kyoto, Japan) equipped with in-line flow scintillation analyzer (Shell Jr. 1000/2000, VA, USA). HPLC solvents consisted of H₂O containing 0.1% trifluoroacetic acid (Solvent A) and acetonitrile containing 0.1% trifluoroacetic acid (Solvent B). A symmetric C-18 column (5.0 μm , 100 Å, 4.6 \times 250 mm, Waters, Milford, MA, USA) was employed with volumetric flow rate of 1 ml/min. HPLC gradient began with a solvent composition of 95% A and 5% B and was followed by a linear gradient of 30%A:70%B from 1 to 25 min, and 30%A:70%B to 5%A:95%B from 25 to 28 min.

2.4. Effect of $[\text{}^{99m}\text{Tc}(\text{OH}_2)_3(\text{CO})_3]^+$ activity and molecule mass ratio

Different volumes of modified dextran solution ranging from 10 to 50 μL with concentration of 1 mg/mL were added to 100 μL

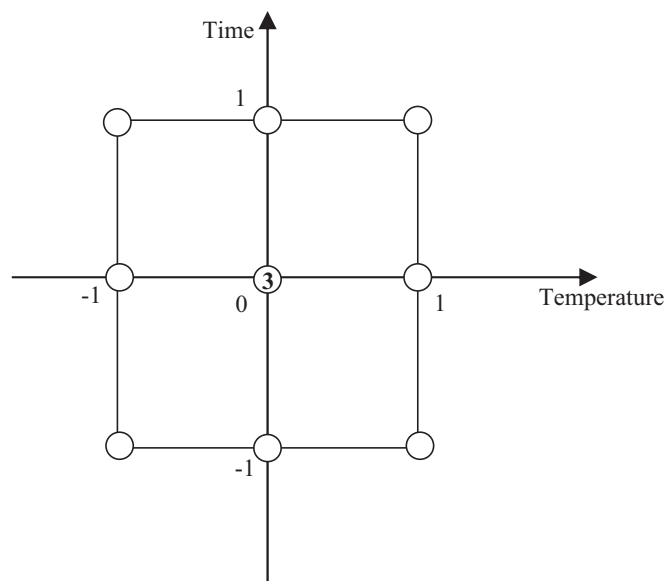


Fig. 2. Distribution of experimental points for statistical analysis according to the three-level full factorial design.

(37 MBq) $[^{99m}\text{Tc}(\text{OH})_2(\text{CO})_3]^+$. Radiolabeling reactions were carried out at 80 °C during 30 min.

2.5. Radiolabeling time and temperature optimization by three-level full factorial design

Effects of radiolabeling time and temperature and their interactions were investigated by three-level full factorial design but any variable could be introduced if appropriate. The assessed levels for time and temperature were 10, 20, 30 min and 70, 85, 100 °C, respectively. They can be represented in codified form (–1, 0, 1) (Fig. 2). Two additional experiments (20 min and 85 °C) in the central point of the experimental region (they are represented in Fig. 2 as number 3 inside the central circle) were included together with nine basic experimental points, in order to evaluate statistical significance of the radiochemical purity pattern. All experiments were performed with 20 µg of 2-propylene–cysteine–dextran (1 mg/ml), 100 µl of $[^{99m}\text{Tc}(\text{OH})_2(\text{CO})_3]^+$ (37 MBq).

2.6. Relation between specific activity and radiochemical purity

Consecutive technetium-99m labeling reactions were conducted using 100 µl of $[^{99m}\text{Tc}(\text{OH})_2(\text{CO})_3]^+$, 74 MBq, with different modified dextran amounts (20, 15, 10, 5, 1, 0.6, 0.3, and 0.1 µg) dissolved in 20 µl. Reaction time and temperature were 30 min and 100 °C, respectively. With the purpose of relating specific activity to radiochemical purity of the radiotracer the mathematical expression was utilized:

$$SA = \frac{ARP}{100M}$$

where SA is specified activity of 2-propylene–cysteine–dextran (MBq/µg), A is activity at the beginning of the reaction (MBq), RP is radiochemical purity and M is modified dextran mass (µg) (British Pharmacopoeia, Zeevaert and Olsen, 2006).

2.7. Radiochemical stability, transchelation toward cysteine and partition coefficient

$^{99m}\text{Tc}(\text{CO})_3$ -2-propylene–cysteine–dextran radiochemical stability was studied over 6 h at room temperature (25 °C) in saline.

Transchelation of the dextran conjugate (1 µM) to cysteine (0.001, 0.01, 0.1 and 1 mM) was also assessed at 37 °C in saline for 90 min (Hnatowich et al., 1994). The cysteine/modified dextran molar ratio varied from 1:1 to 1000:1.

Partition coefficient of the radiotracer was evaluated in octanol/H₂O (5 mL:5 mL) with 200 µl of the radiomolecule preparation. After 15 min of vigorous agitation, the tubes were centrifuged at 5000g for 3 min. Samples of 100 µl (*n*=3) from both phases were measured in a γ counter, and the partition coefficient was expressed as log*P*:

$$\log P = \log \frac{A_{\text{octanol}}}{A_{\text{H}_2\text{O}}}$$

where *A*_{octanol} and *A*_{H₂O} are the activity average in octanol and H₂O phases, respectively.

2.8. Lymphoscintigraphy and ex-vivo uptake in rats

Animals were anesthetized using 25 mg/kg tiletamine hydrochloride associated with 25 mg/kg zolazepam hydrochloride (Zoletil 50, Virbac, São Paulo, Brazil) administered intraperitoneally. Afterwards 0.1 ml (37 MBq) of the radiotracer with the best radiolabeling parameters and yield defined before was injected in the footpad of the left posterior limb.

Images at 90 min post injection were performed in a Mediso Imaging System, Budapest, Hungary, employing a low-energy high-resolution collimator with 256 × 256 × 16 matrix size and 20% energy window set at 140 keV.

A second injection with 0.05 ml vital dye was administered in the same footpad, five minutes before sacrifice time (90 min).

The popliteal region was surgically incised permitting access and removal of the popliteal lymph node. Laparotomy with removal of kidneys and liver was also promptly executed, for simultaneous evaluation. Radioactivity of the specimens was determined by γ-counting. Results were expressed as percentage of injected dose per organ (%ID).

2.9. General descriptive and analytical statistics

Samples were compared by Student's "t" test to a significance level of 5% (*P* < 0.05), employing Statgraphics Plus 5.0 (Statistical Graphics Corp., Fairfax, VA., USA). Analysis of the three-level full factorial design was carried out in Design Expert version 5.0 for Windows (Stat-Ease, Inc., MN, USA). Additional graphics were generated by Microsoft® Office Excel 2003 spreadsheet.

3. Results

3.1. Effect of $[^{99m}\text{Tc}(\text{OH})_2(\text{CO})_3]^+$ activity and molecule mass ratio

Radiolabeling efficiency of $[^{99m}\text{Tc}(\text{OH})_2(\text{CO})_3]^+$ was higher than 99%. Radiochemical species from radiolabeled cysteine–dextran were defined by two radiochromatographic techniques. The impurity $^{99m}\text{TcO}_4^-$ has a *R_f*=1 in the Whatman 1/Acetone paper system as well as in ITLC-SG/ Methanol:HCL (99:1), and the same was true for $[^{99m}\text{Tc}(\text{OH})_2(\text{CO})_3]^+$ in the last procedure. ^{99m}Tc -2-propylene–S–cysteine–dextran did not migrate from the point of sample application (*R_f*=0) in ITLC-SG/Methanol:HCL (99:1) system.

Radiochemical purity for different modified dextran amounts (10, 20, 30, and 50 µg) was 91.6%, 91.8%, 92.9% and 95.0%, respectively.

^{99m}Tc -2-propylene–S–cysteine–dextran and radiochemical impurities were also screened by size-exclusion chromatograph on PD-10 column. Radiolabeled modified dextran was eluted in

Table 1
Experimental matrix and radiochemical yield for each point included in three-level full factorial design.

Temperature (°C)	Time (min)	^{99m} Tc-DC (%)
70	10	79.91
85	10	91.62
100	10	93.25
70	20	88.47
85	20	92.97
100	20	95.62
70	30	90.88
85	30	96.14
100	30	94.46
85	20	93.51
85	20	94.20

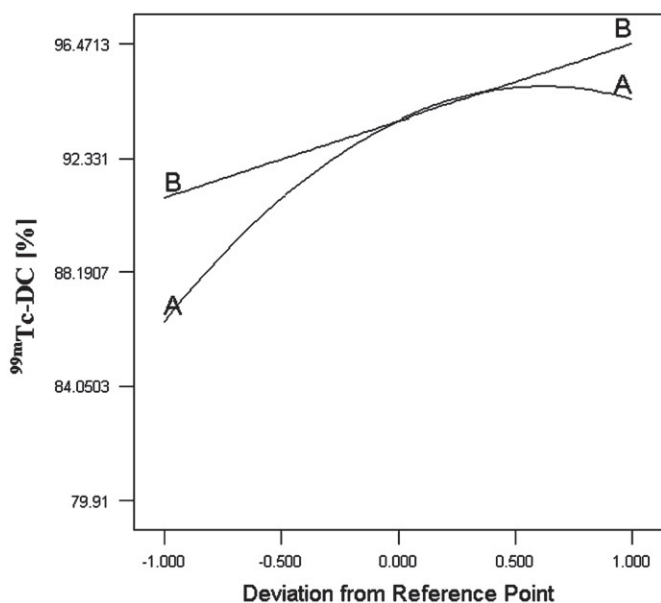


Fig. 3. Perturbation graph for ^{99m}Tc-DC [%]. (A) Temperature (0=85 °C) and (B) Time (0–20 min).

fractions 6–10. Maximum retention fractions for ^{99m}Tc-carbonyl core and for ^{99m}TcO₄⁻ were 17 and 20, respectively.

3.2. Radiolabeling time and temperature optimization

Radiochemical yields for each experimental point included in three-level full factorial design are reproduced in Table 1.

The statistical equation that describes radiochemical yield as a function of reaction time and temperature is:

$${}^{99m}\text{Tc-DC}[\%] = -66.83 + 3.05T + 1.66t - 0.01T^2 - 0.016Tt,$$

where ^{99m}Tc-DC is radiochemical purity of ^{99m}Tc-modified dextran (%), *T* indicates temperature (°C), and *t* radiolabeling time (min).

According to the equation above, time influence on radiochemical yield was linearly positive within the study range (10–30 min). In contrast temperature exhibited quadratic performance, with non-significant increase of the yield between 85 and 100 °C. Improvement was demonstrated only between 70 and 85 °C, of approximately 8% (Fig. 3).

In general when both variables were elevated, radiolabeling yield also increased. At high values of reaction time and temperatures a yield in excess of 95% could be demonstrated.

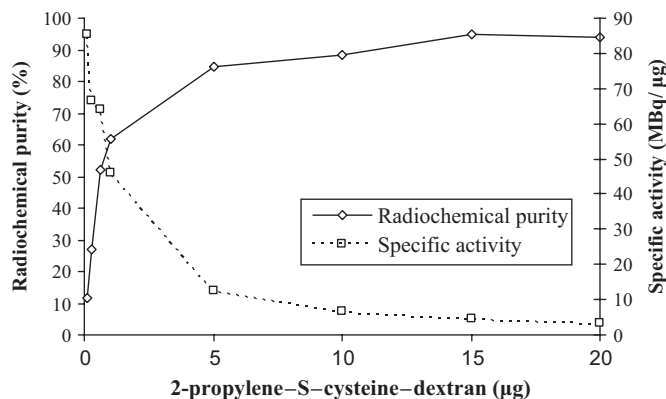


Fig. 4. Influence of polymer mass on radiochemical purity and specific activity.

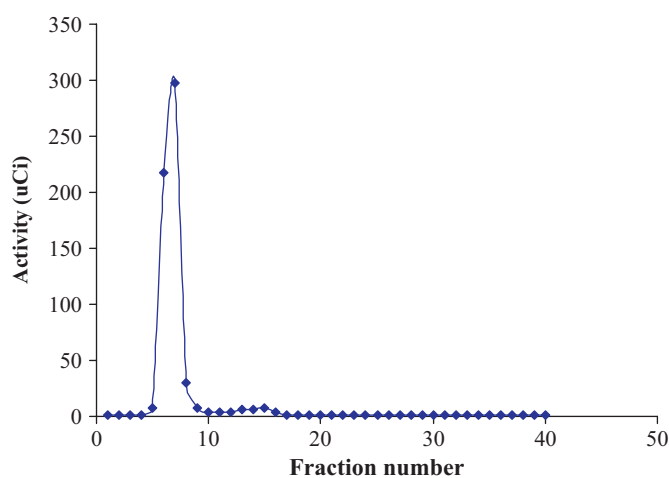


Fig. 5. Size exclusion chromatography in PD-10 to determine ^{99m}Tc-2-propylene-S-cysteine-dextran and impurities (0.5 mL fraction size).

3.3. Relation between specific activity and radiochemical purity

Theoretical specific activity related to radiochemical purity was always considered. A significant decrease in radiochemical purity was observed when 15 µg of the polymer (95%) was reduced to 10 µg (88%), even though specific activity was higher (Fig. 4). These results support utilization of [^{99m}Tc(OH)₂(CO)₃]⁺ activity and cysteine-dextran mass ratio within a range conducting to specific activity of 3–5 MBq/µg.

3.4. Radiochemical evaluation for best radiolabeling conditions

^{99m}Tc-2-propylene-S-cysteine-dextran content was corroborated by gel filtration chromatography in PD-10 column (Fig. 5) and by RP-HPLC (Fig. 6). Best radiolabeling conditions were 30 min reaction time, 100 °C temperature, 20 µg polymer (1 mg/ml) and 100 µl [^{99m}Tc(OH)₂(CO)₃]⁺ (74 MBq). Radiochemical composition under these conditions was 95.0 ± 1.0% ^{99m}Tc-modified dextran, 3.2 ± 0.4% [^{99m}Tc(OH)₂(CO)₃]⁺ and 1.9 ± 0.03% ^{99m}TcO₄⁻.

3.5. Radiochemical stability, transchelation toward cysteine and partition coefficient

Purity levels at the end of radiolabeling reaction (95.0 ± 1.0%) and 6 h later (93.9 ± 1.1%) were statistically similar (*P*=0.237, Student's "t" test, *n*=3).

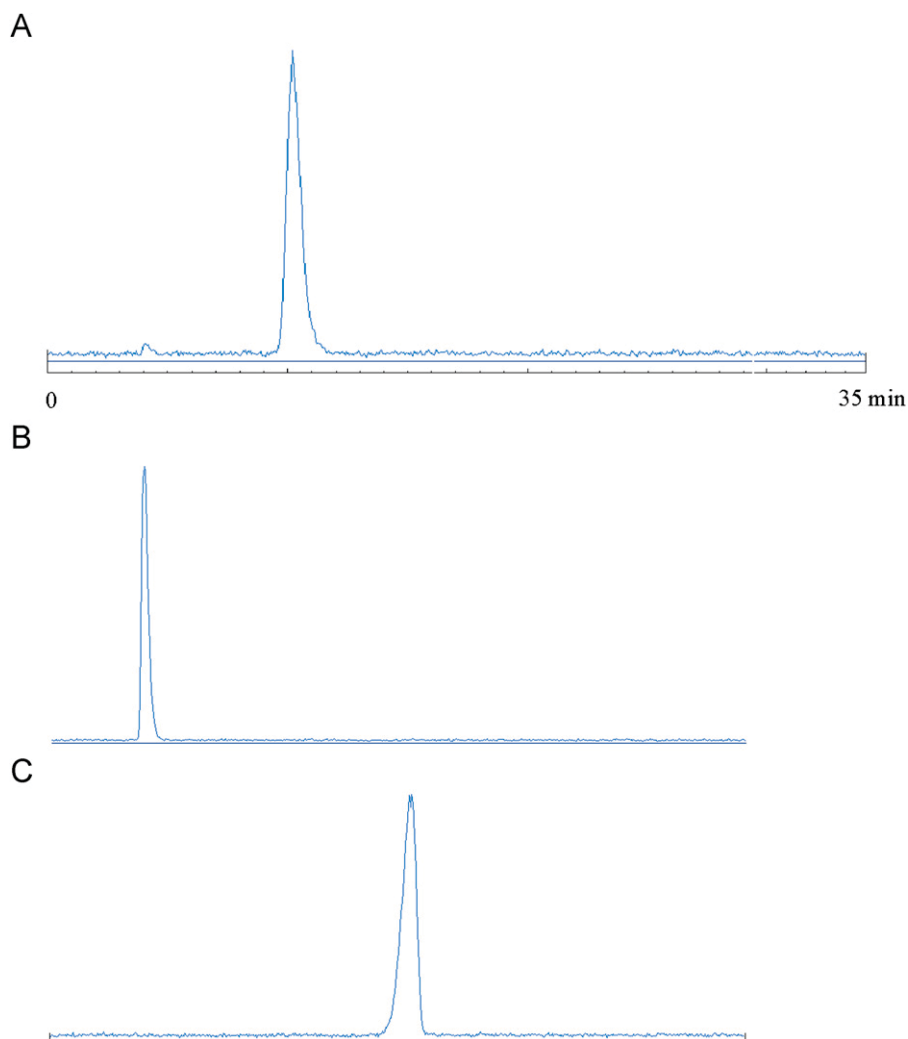


Fig. 6. HPLC profile for ^{99m}Tc -DC and impurities. (A) ^{99m}Tc -2-propylene-S-cysteine-dextran profile, retention time: 10.1 min., (B) $^{99m}\text{TcO}_4^-$ profile, retention time: 4.7 min. and (C) $[\text{}^{99m}\text{Tc}(\text{OH}_2)_3(\text{CO})_3]^+$ profile, retention time: 18 min.

Table 2
Stability of ^{99m}Tc -modified dextran towards cysteine transchelation.

Cysteine concentration (mM)	Transchelation (%)
0	0
0.001	0.923
0.01	1.522
0.1	2.108
1	3.510

Transchelation toward cysteine was inferior to 4%, even at concentrations of this amino acid above the physiological levels (Table 2). Partition coefficient for the radiotracer was $\log P = -2.208$, a value compatible with a hydrophilic molecule.

3.6. Lymphoscintigraphy and ex-vivo uptake study in rats

Lymphoscintigraphy 90 min post injection of the radiotracer elicited a clear image of the popliteal lymph node (Fig. 7). Ex-vivo uptake obtained for the different species was $0.7 \pm 0.2\% \text{ID}$ for popliteal lymph node, $0.5 \pm 0.1\% \text{ID}$ for liver and $2.5 \pm 0.4\% \text{ID}$ for kidneys.

4. Discussion

Radiochemical reactions suffer the impact of the same variables as ordinary chemical reactions, among which the most important ones are molar ratio, temperature, time and concentrations. Specifically for radiotracers used in nuclear medicine, simple protocols and short reaction times are preferred. This became more critical when radioisotopes with short half-life are manipulated.

Radiolabeling temperature is usually governed by intrinsic chemical stability as well as by kinetic details. Molar ratio should be defined taking into consideration high radiochemical purity and specific activity. As a rule, high concentrations improve reaction rate.

For radiopharmaceuticals prepared with $[\text{}^{99m}\text{Tc}(\text{OH}_2)_3(\text{CO})_3]^+$ precursor (Isolink kit), three variables are critical: temperature, time and mass of molecule/ $[\text{}^{99m}\text{Tc}(\text{OH}_2)_3(\text{CO})_3]^+$ activity ratio. The last parameter is equivalent to the molar ratio in common chemical reactions. Reagent concentrations are not considered because Isolink kit is limited in ^{99m}Tc activity (1000 MBq/1 mL) (Decristoforo et al., 2006). In this work, a small constant volume of the non-radioactive molecule containing different masses was used in the experimental optimization process. Thus, molar ratio and reagent concentrations are condensed in a single variable.

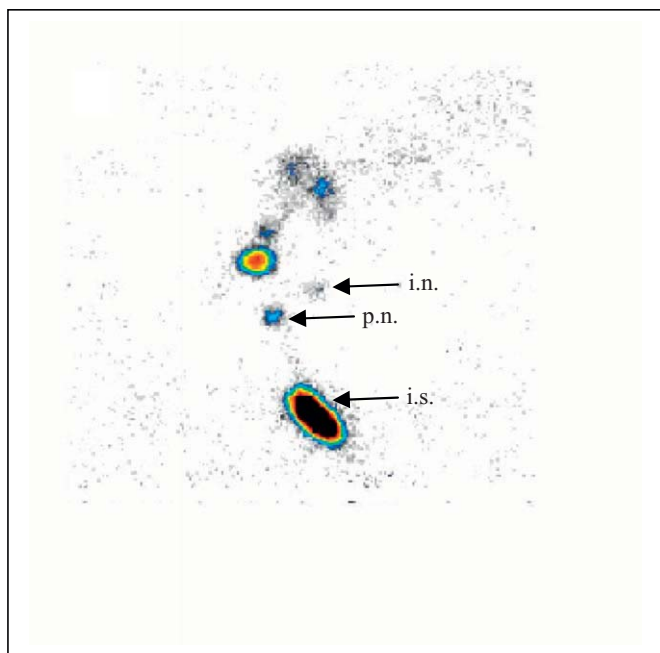


Fig. 7. Lymphoscintigraphy imaging of rat popliteal lymph node after injection into left posterior limb footpad of ^{99m}Tc -2-propylene-S-cysteine-dextran. p.n.: popliteal node; i.n.: inguinal node; i.s.: injection site.

Statistical optimization of pharmaceutical or chemical procedures with two or three variables can be performed in different ways. Available examples are the central composite (Cornelissen et al., 2004) along with three-level designs (Ferreira et al., 2007). One of the pitfalls of statistical strategies is to perform optimization studies in wide experimental domain (many variables with broad ranges), because a mathematical model will be constructed on the basis of just a few empirical points. Thus, the previous knowledge about system under study and its variable constrains can reduce the experimental space and increase the model accuracy.

In our methodology radiolabeling reactions with different molar ratios were carried out at first, while other variables were kept constant. A slight mathematical dependence of radiochemical purity with regard to $[\text{}^{99m}\text{Tc}(\text{OH})_2(\text{CO})_3]^+$ activity and non-radioactive molecule mass ratio was observed. Nevertheless specific activity of the molecule was low, compared to theoretical possibilities.

The next step was to address the effects of time (10–30 min) and temperature (70–100 °C) on radiochemical purity of the ^{99m}Tc -dextran conjugate with low non-radioactive molecule mass/ $[\text{}^{99m}\text{Tc}(\text{OH})_2(\text{CO})_3]^+$ activity ratio, in order to improve specific activity. Variable ranges were selected taking into account thermal stability of dextran as well as common hospital conditions and 99m-technetium half-life time.

Results were consistent with the hypothesis that higher values of both variables increase radiochemical purity, although significant differences were not detected between 85 and 100 °C. As a consequence, 30 min of reaction and 100 °C could be defined as optimum values. The temperature of 100 °C was chosen because it is easier to control in lab conditions.

Finally, non-radioactive molecule mass/ $[\text{}^{99m}\text{Tc}(\text{OH})_2(\text{CO})_3]^+$ activity (74 MBq) ratio was explored. The inferior level of this ratio was deducted from a theoretical molar ratio of 1:1 between two reagents, considering a nominal specific activity of ^{99m}Tc (520,554 Ci mmol⁻¹) (Eckelman et al., 2008).

Modified dextran in optimal conditions (30 min, 100 °C and 74 MBq $[\text{}^{99m}\text{Tc}(\text{OH})_2(\text{CO})_3]^+$ /15–20 µg) exhibited radiochemical purity around 95% and 3–5 MBq/µg. These results are better than with other ^{99m}Tc -dextran conjugates (0.0082 MBq/µg)

(Matsunaga et al., 2005). Generally, best conditions for radiolabeling could be defined by the interception of radiochemical purity and specific activity curves (Fig. 4). However, it must not overlook that radiochemical purity at this point should achieve acceptable values for regulatory agencies, as well as it should not adversely interfere with radiotracer biological performance.

High purity of radiopharmaceuticals radiolabeled with $[\text{}^{99m}\text{Tc}(\text{OH})_2(\text{CO})_3]^+$ is further advantageous, by minimizing the image background effect due to the binding of $[\text{}^{99m}\text{Tc}(\text{OH})_2(\text{CO})_3]^+$ to proteins, specifically albumin by means of histidine and cysteine moieties (Biechlin et al., 2005).

It is worth emphasizing that the statistical approach here adopted paves the way for reduced optimization steps, and streamlining of the entire labeling routine in future studies for other technetium radiotracers based on cysteine-dextran conjugates.

Once optimal values for the three principal parameters were established, radiochemical stability at room temperature and physiological conditions required attention. ^{99m}Tc -2-propylene-S-cysteine-dextran is stable at room temperature and concentrations of cysteine above physiological levels (264 µM) (Obled et al., 2004). More than 95% of the radioactivity remained associated with the conjugate in such circumstances, similarly to other radiolabeled dextrans (Du et al., 2000). Such confirmation encourages the development and clinical testing of new radiopharmaceuticals based on this radiocARRIER.

Imaging conducted with the radiotracer was perfectly adequate for popliteal lymph node visualization (Fig. 7). The uptake of ^{99m}Tc -2-propylene-S-cysteine-dextran in this ganglion and the observed values for a chemically analogous radiotracer, ^{99m}Tc -Dextran-500 ($0.55 \pm 0.14\%$ ID) (Fernández-Núñez et al., 2009) were similar, using the same experimental conditions and animal model. Therefore, it was demonstrated that ^{99m}Tc -Dextrans in a 16.6–500 kDa range do not induce changes in popliteal lymph node uptake.

High kidney uptake ($2.5 \pm 0.4\%$ ID) was noticed, even though injection was local and not intravenous, probably due to significant hydrophilicity of the agent and relative low molecular weight (16.6 kDa). The kidney uptake of the tracer included in this study was 19.2 fold higher than ^{99m}Tc -Dextran-500 ($0.13 \pm 0.05\%$ ID). On the other hand, the liver uptake ($0.5 \pm 0.1\%$ ID) was also higher when it was compared with ^{99m}Tc -Dextran-500 ($0.06 \pm 0.05\%$ ID) (Fernández-Núñez et al., 2009). Thus, the renal and hepatic uptakes of hydrophilic ^{99m}Tc -Dextran derivatives used as lymphoscintigraphic agents seem to be governed by the molecular weight. This is an indirect evidence of faster injection site migration for dextrans with low molecular weights.

The traditional technetium radiochemical method for dextrans, including ^{99m}Tc -Dextran-500, it is based on 99m-technetium reduction with stannous chloride and coupling of this isotope to two adjacent hydroxyl groups in dextran backbone. Only two of five technetium coordination sites are used for binding technetium to the polymer (Henze et al., 1982). As a consequence, this approach has two main drawbacks: contamination with technetium colloid and technetium transchelation in biological fluids due to the weak chelating capacity of hydroxyl groups (Matsunaga et al., 2005). The utilization of cysteine-dextran conjugates and *fac*- $[\text{}^{99m}\text{Tc}(\text{OH})_2(\text{CO})_3]^+$ synthon for dextran radiolabeling overcomes these deficiencies.

5. Conclusion

Statistical strategy for radiolabeling optimization of cysteine-dextran conjugate with technetium tricarbonyl core was convenient and successful, using a three-level factorial design. Specific activity reached was 5 MBq/µg, which exceeds previously reported results.

As efficient lymph node radiotracer could be prepared, and the possibility of extending the benefits of such routine for additional radiopharmaceuticals that display cysteine–dextran as carrier is anticipated.

Acknowledgments

The authors are indebted to the National Commission for Nuclear Energy (CNEN, São Paulo, Brazil), National Counsel of Technological and Scientific Development (CNPq, Brasília, Brazil) and the International Atomic Energy Agency (IAEA, Vienna, Austria) for scientific grants. The first author gratefully acknowledges his wife, Relma Tavares de Oliveira Fernández, and Oscar Pérez Fernández for the inspiration to write this paper.

References

- Alberto, R., 2005. New organometallic technetium complexes for radiopharmaceutical imaging. *Top. Curr. Chem.* 252, 1–41.
- Avril, N., Weber, W., Schwaiger, M., 2005. Positron emission tomography: significance for preoperative *n*-staging. In: Schauer, A.J., Becker, W., Reiser, M., Possinger, K. (Eds.), *The Sentinel Lymph Node Concept*. Springer, Berlin, pp. 31–37.
- Bensimhon, L., Métayé, T., Guilhot, J., Perdrisot, R., 2008. Influence of temperature on the radiochemical purity of ^{99m}Tc-colloidal rhenium sulfide for use in sentinel node localization. *Nucl. Med. Commun.* 29, 1015–1020.
- Biechlin, M.L., du Moulinet d'Hardemare, A., Fraysse, M., Gilly, F.N., Bonmartin, A., 2005. Improvement in radiolabelling proteins with the ^{99m}Tc-tricarbonyl-core [^{99m}Tc(CO)₃]⁺, by thiol-derivatization with iminothiolane: application to γ -globulins and annexin V. *J. Label Compd. Radiopharm.* 48, 873–885.
- Castellanos Gil, E., Iraizoz Colarte, A., El Ghzaoui, A., Durand, D., Delarbre, J.L., Bataille, B., 2008. A sugarcane native dextran as an innovative functional excipient for the development of pharmaceutical tablets. *Eur. J. Pharm. Biopharm.* 68, 319–329.
- Cornelissen, B., Thonissen, T., Kersemans, V., Van De Wiele, C., Lahorte, C., Dierckx, R.A., Slegers, G., 2004. Influence of farnesyl transferase inhibitor treatment on epidermal growth factor receptor status. *Nucl. Med. Biol.* 31, 679–689.
- de Belder, A.N., 1996. Medical applications of dextran and its derivatives. In: Dumitriu, S. (Ed.), *Polysaccharides in Medicinal Applications*. Marcel Dekker Inc., New York, pp. 505–524.
- Decristoforo, C., Faintuch-Linkowski, B., Rey, A., von Guggenberg, E., Rupprich, M., Hernandez-Gonzales, I., Teodoro, R., Haubner, R., 2006. [^{99m}Tc]HYNIC-RGD for imaging integrin $\alpha v \beta 3$ expression. *Nucl. Med. Biol.* 33, 945–952.
- Du, J., Marquez, M., Hiltunen, J., Nilsson, S., Holmberg, A.R., 2000. Radiolabeling of dextran with rhenium-188. *Appl. Radiat. Isot.* 53, 443–448.
- Eckelman, W.C., Volkert, W.A., Bonardi, M., 2008. True radiotracers: are we approaching theoretical specific activity with Tc-99m and I-123? *Nucl. Med. Biol.* 35, 523–527.
- El-Maraghi, R.H., Kielar, A.Z., 2008. PET vs sentinel lymph node biopsy for staging melanoma: a patient intervention, comparison, outcome analysis. *J. Am. Coll. Radiol.* 5, 924–931.
- Fernández-Núñez, E.G., Faintuch, B.L., Teodoro, R., Wiecek, D.P., Martinelli, J.R., da Silva, N.G., Castanheira, C.E., de Oliveira Filho, R.S., Pasqualini, R., 2009. Influence of colloid particle profile on sentinel lymph node uptake. *Nucl. Med. Biol.* 36, 741–747.
- Ferreira, S.L.C., Bruns, R.E., Ferreira, H.S., Matos, G.D., David, J.M., Brandão, G.C., da Silva, E.G.P., Portugal, L.A., dos Reis, P.S., Souza, A.S., dos Santos, W.N.L., 2007. Box-Behnken design: an alternative for the optimization of analytical methods. *Anal. Chim. Acta* 597, 179–186.
- Heinze, T., Michealis, N., Hornig, S., 2007. Reactive polymeric nanoparticles based on unconventional dextran derivatives. *Eur. Polym. J.* 43, 697–703.
- Henze, E., Robinson, G.D., Kuhl, D.E., Schelbert, H.R., 1982. Tc-99m Dextran: a new blood-pool-labeling agent for radionuclide angiocardiology. *J. Nucl. Med.* 23, 348–353.
- Hnatowich, D.J., Virzi, F., Fogarasi, M., Rusckowski, M., Winnard, P., 1994. Can a cysteine challenge assay predict the in vitro behavior of ^{99m}Tc-labeled antibodies? *Nucl. Med. Biol.* 21, 1035–1044.
- Karagiorgou, O., Patsis, G., Pelecanou, M., Raptopoulou, C.P., Terzis, A., Siatra-Papastaikoudi, T., Alberto, R., Pirmettis, I., Papadopoulos, M., 2005. S-(2-(2'-pyridyl)ethyl)cysteamine and S-(2-(2'-pyridyl)ethyl)-D,L-homocysteine as ligands for the "fac-[M(CO)₃]" (M=Re, ^{99m}Tc) core. *Inorg. Chem.* 44, 4118–4120.
- Khalikova, E., Susi, P., Korpela, T., 2005. Microbial dextran-hydrolyzing enzymes: fundamentals and applications. *Microbiol. Mol. Biol. Rev.* 69, 306–325.
- Krishnamoorthi, S., Mal, D., Singh, R.P., 2007. Characterization of graft copolymer based on polyacrylamide and dextran. *Carbohydr. Polym.* 69, 371–377.
- Kyprianidou, P., Tsoukalas, C., Patsis, G., Papagiannopoulou, D., Nikolić, N., Janković, D., Djokić, D., Raptopoulou, C.P., Pelecanou, M., Papadopoulos, M., Pirmettis, I., 2009. Rhenium(I) and technetium-99m(I) fac-tricarbonyl complexes with 4-(imidazolin-2-yl)-3-thiabutanoic acid derivatives as tridentate ligands: synthesis and structural characterization. *Polyhedron* 28, 3171–3176.
- Matsunaga, K., Hara, K., Imamura, T., Fujioka, T., Takata, J., Karube, Y., 2005. Technetium labeling of dextran incorporating cysteamine as a ligand. *Nucl. Med. Biol.* 32, 279–285.
- Mundwiler, S., Waibel, R., Spingler, B., Kunze, S., Alberto, R., 2005. Picolyamine-methylphosphonic acid esters as tridentate ligands for the labeling of alcohols with the fac-[M(CO)₃]⁺ core (M=^{99m}Tc, Re): synthesis and biodistribution of model compounds and of a ^{99m}Tc-labeled cobinamide. *Nucl. Med. Biol.* 32, 473–484.
- Obled, C., Papet, I., Breuillé, D., 2004. Sulfur-containing amino acids and glutathione in diseases. In: Cynobe, L.A. (Ed.), *Metabolic and Therapeutic Aspects of Amino Acids in Clinical Nutrition 2nd Edition*. CRC Press, Florida, pp. 667–688.
- Schauer, A.J., Becker, W., Reiser, M., Possinger, K., 2005. Specific developments in sentinel node labeling using ^{99m}Tc-colloids. In: Schauer, A.J., Becker, W., Reiser, M., Possinger, K. (Eds.), *The Sentinel Lymph Node Concept*. Springer, Berlin, pp. 59–69.
- Šević, S.S., Pantelić, D., 2008. Biopolymer holographic diffraction gratings. *Opt. Mater.* 30, 1205–1207.
- Sun, G., Chu, C.C., 2006. Synthesis, characterization of biodegradable dextran–allyl isocyanate–ethylamine/polyethylene glycol–diacrylate hydrogels and their in vitro release of albumin. *Carbohydr. Polym.* 65, 273–287.
- van Staveren, D., Benny, P., Waibel, R., Kurz, P., Pak, J.-K., Alberto, R., 2005. S-functionalized cysteine: powerful ligands for the labelling of bioactive molecules with triaquatricarbonyltechnetium-99m(1+) ([^{99m}Tc(OH₂)₃(CO)₃]⁺). *Helv. Chim. Acta* 88, 447–460.
- Wallace, A.M., Hoh, C.K., Vera, D.R., Darrah, D.D., Schulteis, G., 2003. Lymphoseek: a molecular radiopharmaceutical for sentinel node detection. *Ann. Surg. Oncol.* 10, 531–538.
- Zeevaert, J.R., Olsen, S., 2006. Recent trends in the concept of specific activity: Impact on radiochemical and radiopharmaceutical producers. *Appl. Radiat. Isotop.* 64, 812–814.
- Zornoza, G., Garcia-Velloso, M.J., Sola, J., Regueira, F.M., Pina, L., Beorlegui, C., 2004. ¹⁸F-FDG PET complemented with sentinel lymph node biopsy in the detection of axillary involvement in breast cancer. *Eur. J. Surg. Oncol.* 30, 15–19.